J Mol Model (2011) 17:3209–3217
DOI 10.1007/s00894-010-0941-z

ORIGINAL PAPER

Formation of the Vilsmeier-Haack complex: the performance of different levels of theory

Gül Altınbaş Özpınar · Dieter E. Kaufmann · Timothy Clark

Received: 24 November 2010 / Accepted: 20 December 2010 / Published online: 2 March 2011

Abstract Because of discrepancies in the available experimental data, an extensive theoretical investigation of the formation of the Vilsmeier-Haack (VH) complex has been carried out. The barriers to complex formation calculated using eight different density functional methods (BLYP, B2-PLYP, B3LYP, B3PW91, MPW1K, M06-2X, and PBE1PBE), MP2, and extrapolation techniques (CBS-QB3, G3B3) with several basis sets (6−31+G**, 6−311++G**, 6−311+(3df,2p), aug-cc-pVDZ, and aug-cc-pVTZ) were compared with experimental data. For the overall reaction, MP2/aug-cc-pVDZ and M06-2X/6−31+G(d,p) perform best compared to the CBS techniques. The results help clarify some open mechanistic questions.

Keywords Ab initio · DFT · Vilsmeier reaction

Electronic supplementary material The online version of this article (doi:10.1007/s00894-010-0941-z) contains supplementary material, which is available to authorized users.

G. A. Özpınar · T. Clark (✉)
Computer-Chemie-Centrum, Friedrich-Alexander-Universität Erlangen-Nürnberg,
Nägelsbachstrsse 25,
91052 Erlangen, Germany
e-mail: clark@chemie.uni-erlangen.de

T. Clark
e-mail: Tim.Clark@chemie.uni-erlangen.de

G. A. Özpınar · T. Clark
Excellence Cluster Engineering of Advanced Materials, Friedrich-Alexander-Universität Erlangen-Nürnberg,
Nägelsbachstrasse 49b,
91052 Erlangen, Germany

G. A. Özpınar
Department of Chemistry, Faculty of Science and Letters,
Kırklareli University,
Kavaklı Campus,
39050 Kırklareli, Turkey

D. E. Kaufmann
Technische Universität Clausthal, Institut für Organische Chemie,
Leibnizstrasse 6,
38678 Clausthal-Zellerfeld, Germany

Introduction

The Vilsmeier-Haack (VH) reaction [1], originally reported in 1927, has long been an important synthetic reaction. It has been used extensively for formylation and the synthesis of biologically active heterocyclic compounds [2–7]. In general, the reaction proceeds via formation of a complex between *N*,*N*-dimethylformamide (DMF) and $POCl_3$ (Fig. 1). This electrophilic adduct is instrumental in introducing an aldehyde group into activated aromatic compounds since it decomposes readily in contact with water. It has been reported that the rate-determining step of the formylation reaction is either the attack of this electrophilic adduct on the aromatic substrate or the formation of the adduct itself, depending on the reactivity of aromatic substrate [8]. Three different types of Vilsmeier complex structure have been proposed, as shown in Fig. 1. The covalent structure I can be ruled out based on infrared spectra [9, 10]. The spectroscopic [11] and chemical [12, 13] evidence suggests one of the ionic structures II or III.

Martin et al. [14] studied the mechanism of the complex formation in dichloromethane at different temperatures by nuclear magnetic resonance spectroscopy and reported a free energy of activation of 15.3 kcal mol^{-1} at 313 K and that the reaction follows second-order kinetics. They suggested that the complex structures were in equilibrium with the reagents. Another kinetic investigation of the complex formation was

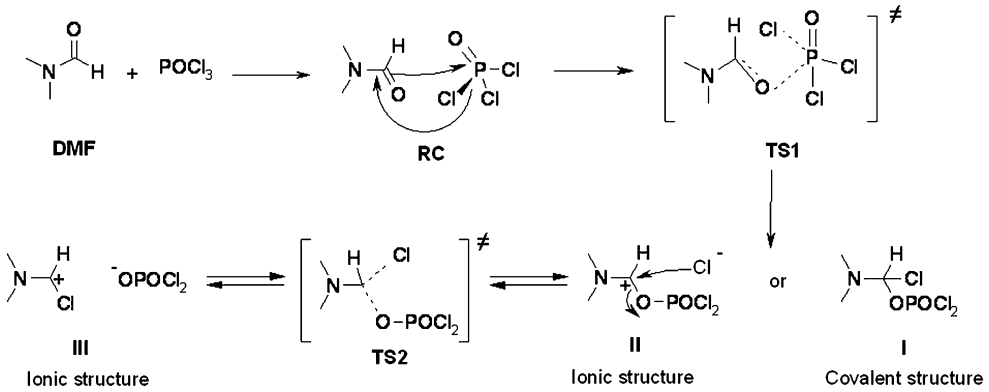

Fig. 1 The proposed mechanism of Vilsmeier-Haack (VH) complex formation. (RC = Reactant complex and TS = transition state)

carried out by Alunni et al. [8], also at different temperatures in dichloroethane. They also observed second-order kinetics for the formation of the complex. According to their results, the reaction enthalpy and entropy of the formation were found to be -13.7 kcal mol^{-1} and -38.6 kcal mol^{-1}, respectively, and the activation parameters were $\Delta H^{\neq}$= 15.8 kcal mol^{-1} and $\Delta S^{\neq}$=-20.7 cal mol^{-1} K^{-1}, which corresponds to a free energy of activation with 22.3 kcal mol^{-1} at 313 K. However, they also noted a serious disagreement between their values and those of Martin et al. that cannot be ascribed entirely to the different experimental conditions. Recently, Dyer et al. [15] also performed a kinetic investigation of the Vilsmeier reaction. Their suggested mechanism is that the carbonyl oxygen makes a new single bond with phosphorous when the P-Cl single bond breaks in the first step to form the ionic structure II. A rearrangement is then suggested to occur to form structure III in the second step. They calculated the kinetic data for each step at different temperatures in dichloromethane. Their computed activation parameters were $\Delta H^{\neq}$=0.81 kcal mol^{-1} $\Delta S^{\neq}$=-68.83 cal mol^{-1} K^{-1} for the first step, in which the reaction follows the second-order kinetics, and $\Delta H^{\neq}$=12.47 kcal mol^{-1} $\Delta S^{\neq}$=-33.92 cal mol^{-1} K^{-1} for the second step (first-order kinetics). They also reported the reaction enthalpies of the first and second steps to be −1.82 and −2.20 kcal mol^{-1}, which corresponds to a total reaction enthalpy of −4.02 kcal mol^{-1}. However, they reported that the complex formation follows first-order kinetics since the second step of the complex formation is rate determining, in disagreement with the earlier results of Alunni et al. [8] and Martin et al. [14], both concerning the reaction kinetics and the activation enthalpies.

In view of the experimental ambiguities and because we are unaware of theoretical work on the Vilsmeier formylation, we now report a high-level ab initio and density-functional theory (DFT) study of the mechanism of Vilsmeier-Haack complex. Our purpose in modeling the mechanism using reference (ab initio extrapolation) methods is twofold; to resolve the differences between the experimental studies and to define the performance of computationally more economical DFT techniques and MP2 for such processes.

Computational methods

Calculations were performed with the Gaussian 03 [16] and Gaussian 09 [17] program packages. In order to obtain chemically accurate theoretical gas-phase thermochemical energies, CBS−QB3 [18–20] and G3B3 [21] were used. CBS−QB3 energies of the complex structures II and III in solvent were corrected for solvent effects (in dichloroethane) using the SMD [22] solvation model. The functionals we have tested are the BLYP [23–25], Grimme's pertubatively corrected density functional B2-PLYP [26], B3LYP [25, 27], B3PW91 [27, 28], PBE1PBE [29], the hybrid-GGA MPW1K [30, 31] and the hybrid meta-GGA M06-2X [32]. For comparison, we have also used second-order Møller-Plesset theory (MP2) [33] to calculate the activation barrier of the first step. The 6−31+G**, 6−311++G**, 6−311+G (3df,2p), aug−cc−pVDZ, and aug−cc−pVTZ basis sets [34–40] were used. Analytical computations of vibrational frequencies within the harmonic approximation were used to characterize the stationary points. Thermal corrections to the zero point energy (ZPE), enthalpy, and entropy were calculated at 298.15 K and 1 atm. In addition to using the SMD solvation model, solvent effects using dichloroethane were also taken into account by performing single-point calculations on the gas-phase geometries using the polariz-

Table 1 CBS-QB3 energies (kcal mol^{-1}) of Vilsmeier complex structure III relative to II

	III
Gas phase, 0 K	4.87
Gas phase, 298 K	4.31
Dichloroethane, 298 K	−8.22
Dicholoromethane, 298 K	−8.34

Table 2 Calculated enthalpies (kcal mol^{-1}) of RC (ΔH_{RC}), TS1 ($\Delta H^{\neq}$), and complex II (ΔH_{II}) relative to the reactants. The reference gas-phase energies are simply the mean of the values calculated with CBS-QB3 and G3B3. The MUE is the mean absolute error for ΔH_{RC}, $\Delta H^{\neq}$ and ΔH_{II}

	ΔH_{RC}	$\Delta H^{\neq}$	ΔH_{II}	Error ΔH_{RC}	Error $\Delta H^{\neq}$	Error ΔH_{II}	MUE
CBS−QB3	−5.60	26.13	−1.19				
G3B3	−5.40	26.32	−1.24				
Reference							
	−5.50	26.23	−1.22				
BLYP							
6−31+G(d,p)	−0.52	28.79	12.26	−4.98	−2.57	−13.48	7.01
6−311++(d,p)	−0.98	28.04	12.18	−4.52	−1.82	−13.40	6.58
6−311+G(3df,2p)	−0.51	30.05	10.18	−4.99	−3.83	−11.40	6.74
B2-PLYP							
6−31+G(d,p)	−2.29	36.20	2.88	−3.21	−9.98	−4.10	5.76
6−311++(d,p)	−2.90	35.83	5.92	−2.60	−9.61	−7.14	6.45
6−311+G(3df,2p)	−2.09	36.66	3.25	−3.41	−10.44	−4.47	6.10
B3LYP							
6−31+G(d,p)	−1.61	32.41	8.33	−3.89	−6.19	−9.55	6.54
6−311++(d,p)	−2.01	32.04	8.07	−3.49	−5.82	−9.29	6.20
6−311+G(3df,2p)	−1.56	33.34	5.96	−3.94	−7.12	−7.18	6.08
aug-cc-pVDZ	−1.04	29.92	11.06	−4.46	−3.70	−12.28	6.81
aug-cc-pVTZ	−0.61	33.16	10.35	−4.89	−6.94	−11.57	7.80
B3PW91							
6−31+G(d,p)	−0.79	32.58	7.37	−4.71	−6.36	−8.59	6.55
6−311++(d,p)	−1.43	32.21	6.95	−4.07	−5.99	−8.17	6.07
6−311+G(3df,2p)	−0.81	32.92	7.59	−4.69	−6.70	−8.81	6.73
aug-cc-pVDZ	−0.17	29.81	10.18	−5.33	−3.59	−11.40	6.77
aug-cc-pVTZ	0.17	33.01	9.61	−5.67	−6.79	−10.83	7.76
PBE1PBE							
6−31+G(d,p)	−2.66	29.74	3.50	−2.84	−3.52	−4.72	3.69
6−311++(d,p)	−3.31	29.41	3.08	−2.19	−3.19	−4.30	3.22
6−311+G(3df,2p)	−2.56	29.82	3.71	−2.94	−3.60	−4.93	3.82
aug-cc-pVDZ	−1.93	26.83	6.27	−3.57	−0.60	−7.49	3.89
aug-cc-pVTZ	−1.38	30.04	5.79	−4.12	−3.82	−7.01	4.98
MPW1K							
6−31+G(d,p)	−2.62	31.37	1.82	−2.88	−5.15	−3.04	3.69
6−311++(d,p)	−3.26	31.16	1.32	−2.24	−4.94	−2.54	3.24
6−311+G(3df,2p)	−2.40	31.38	1.98	−3.10	−5.16	−3.20	3.82
aug-cc-pVDZ	−2.30	28.31	4.94	−3.20	−2.09	−6.16	3.81
aug-cc-pVTZ	−1.57	31.69	4.24	−3.93	−5.47	−5.46	4.95
MO6-2X							
6−31+G(d,p)	−6.45	23.49	−3.43	0.95	2.74	2.22	1.97
6−311++(d,p)	−7.39	22.89	−4.27	1.89	3.34	3.06	2.76
6−311+G(3df,2p)	−6.20	24.16	−3.23	0.70	2.07	2.02	1.59
aug-cc-pVDZ	−5.41	20.96	−0.41	−0.09	5.27	−0.81	2.05
aug-cc-pVTZ	−5.43	24.38	−1.18	−0.07	1.85	−0.03	0.65
MP2							
6−31+G(d,p)	−6.28	28.61	−4.11	0.78	−2.39	2.90	2.02
6−311++(d,p)	−6.79	28.50	−5.85	1.29	−2.28	4.64	2.73
6−311+G(3df,2p)	−5.72	25.83	−3.14	0.22	0.40	1.93	0.85
aug-cc-pVDZ	−6.31	20.67	−2.75	0.81	5.56	1.54	2.63

Table 3 Calculated enthalpies (kcal mol^{-1}) of RC (ΔH_{RC}), TS1 ($\Delta H^{\neq}$), and complex II (ΔH_{II}) relative to the reactants in dichloroethane. The differences of the calculated activation ($\Delta\Delta H^{\neq}$) and reaction ($\Delta\Delta H$) enthalpies from the experimental data reported by Alunni et al. [8] and by Dyer et al. [15], respectively, are given in parentheses

Computational levels	ΔH_{RC}	$\Delta H_{TS1}^{\neq}$	$\Delta\Delta H^{\neq}$	ΔH_{II}	$\Delta\Delta H$
M06−2X/6−31+G(d,p)	−3.17	18.51	2.71	−0.82	1.00
M06−2X/6−311+G(3df,2p)	−3.00	19.63	3.83	−0.68	1.14
M062X/aug–cc–pVDZ	−2.35	16.32	0.52	1.15	2.97
M062X/aug–cc–pVTZ	−2.24	19.91	4.11	0.47	2.29
MP2/6−31+G(d,p)	−1.68	25.65	9.85	−0.02	1.80
MP2/6−311+G(3df,2p)	−1.33	22.72	6.92	0.47	2.29
MP2/aug-cc-pVDZ	−2.10	17.56	1.76	0.86	2.68

able continuum (overlapping spheres) model [41] (PCM). Thermodynamic corrections obtained from frequency calculations in the gas phase were added to the electronic energy plus solvation free energy obtained from single point PCM calculations in order to compute ZPE corrected energy, enthalpy, and Gibbs energy values in solution.

Results

The stabilities of complexes II and III (Table 1) were evaluated by comparing the calculated CBS−QB3 energies in the gas phase and solution. Complex II is 4.31 kcal mol^{-1} more stable than III in the gas phase, whereas it is 8.22 and 8.34 kcal mol^{-1} less stable in dichloroethane and dichloromethane, respectively. This indicates that complex III is favored in solution, which agrees with the experimental observations [8, 11–13].

The performance of different density functionals and MP2 relative to the reference calculations for the gas phase

Table 2 shows the calculated activation and reaction enthalpies for the first step. The CBS-QB3 and G3B3 methods agree within close limits for all species calculated and can be considered to represent reference gas-phase data. The mean absolute errors (MUE) of the DFT functionals and MP2 are also given in Table 2. The most popular functionals, B3LYP and B3PW91, used with the aug-cc-pVTZ basis set give the largest deviations (MUE=7.80 and 7.76 kcal mol^{-1}, respectively) from the reference data and also underestimate the reaction enthalpy by an average of −9.97 and −9.56 kcal mol^{-1}, respectively. BLYP performs better in predicting the activation barrier than B3LYP and B3PW91 with an average error of −2.74 kcal mol^{-1}. However, it gives the largest average error (−12.76 kcal mol^{-1}) for the reaction enthalpy. The average MUEs of the BLYP, B3LYP, and B3PW91 functionals are 6.78, 6.69, and 6.78 kcal mol^{-1}, respectively. For the activation enthalpy, the B2-PLYP functional performs even less well than the popular functionals with an average error of −10.01 kcal mol^{-1}, but better for reaction enthalpy (average error of −5.24 kcal mol^{-1}). However, its overall average MUE is still quite significant (6.10 kcal mol^{-1}). PBE1PBE and Truhlar´s hybrid method, MPW1K show similar deviations from the reference data. Their average MUEs are 3.92 and 3.90 kcal mol^{-1}, respectively, better than the DFT functionals mentioned above. On

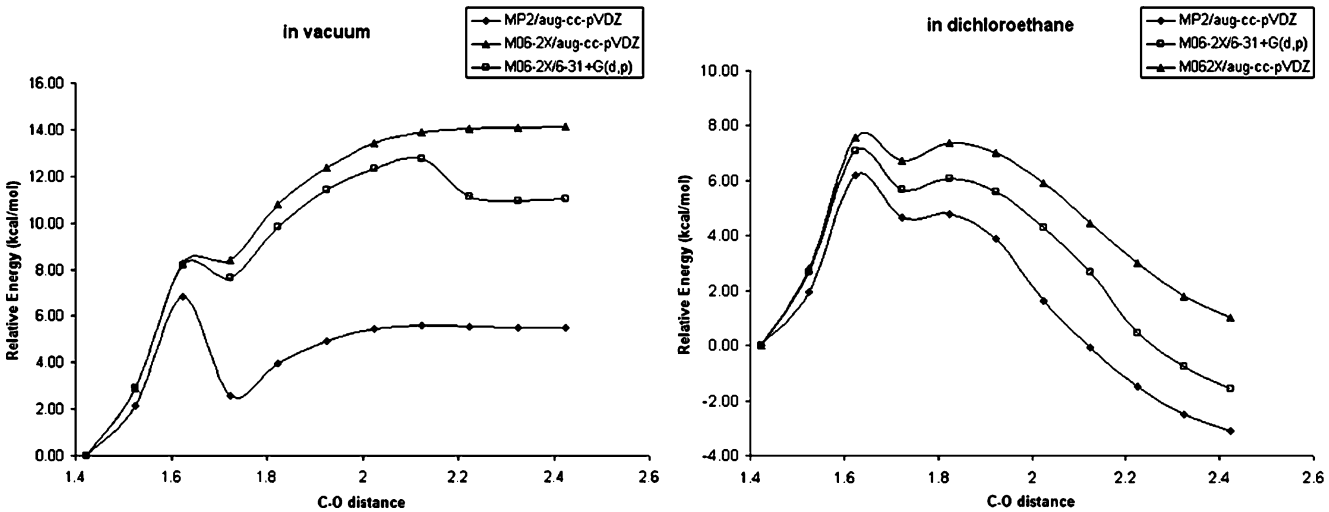

Fig. 2 Potential energy scans (PESs) for the rearrangement step

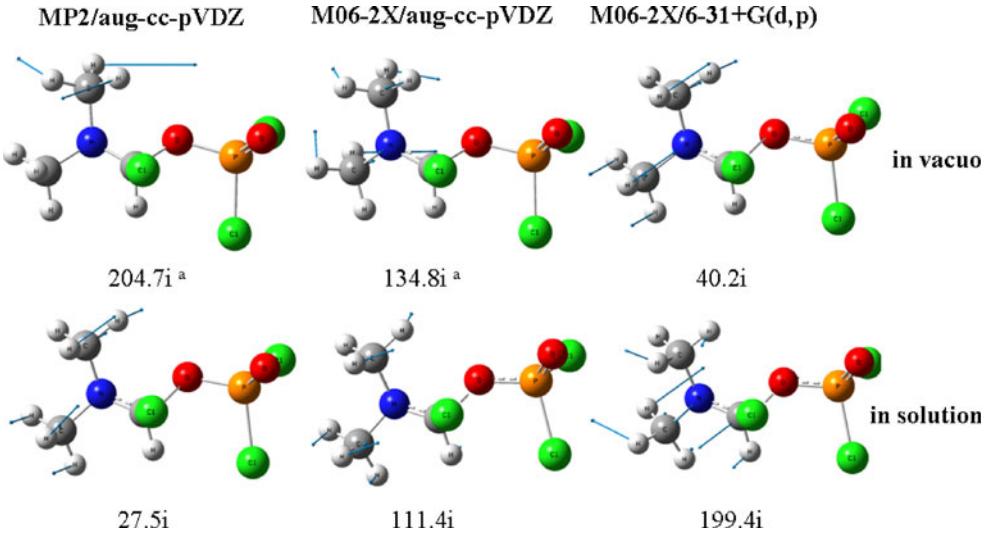

Fig. 3 Imaginary frequencies of third points on the potential energy scans ([a]: obtained from full transition state optimization)

the other hand, Truhlar´s other hybrid-meta method, M06-2X has the lowest MUE (0.65 kcal mol^{-1}) when used with aug-cc-pVTZ and performs the best overall (average MUE=1.84 kcal mol^{-1}) of the DFT functionals investigated. It predicts the activation and reaction enthalpies with average errors of 3.05 and 1.29 kcal mol^{-1}, respectively. MP2 gives the best estimation in the activation barrier (average error=0.26 kcal mol^{-1}), but its average MUE (2.08 kcal mol^{-1}) is 0.24 kcal mol^{-1} higher than that of the M06-2X density functional technique. MP2/6−311+G(3df,2p) and M06-2X/aug-cc-pVTZ perform remarkably well with MUEs of 0.85 kcal mol^{-1}. An adequate basis set is important 6-311+G(3df,2p) and aug-cc-pVTZ perform significantly better than aug-cc-pVDZ.

The calculated solvent effect and comparison with experimental data

The above calculations all refer to the gas phase, whereas the reaction was carried out in dichloroethane or dichloromethane. We therefore considered the solvent effect by calculating the activation enthalpies of the first step using self-consistent reaction field theory. We chose dichloroethane as solvent since it and dichloromethane gave similar stabilities for the ionic complexes (Table 1). The results are listed in Table 3.

Generally, calculations with the aug-cc-pVDZ basis set agree best with the experimental activation energy. The barriers in dichloroethane for MP2 and M06-2X with aug-cc-pVDZ differ only 1.76 and 0.52 kcal mol^{-1} from the experimental value reported by Alunni et al. [8], respectively. The results obtained with the 6−31+G(d,p) basis set vary strongly with the computational method used. M06-2X/6-31+G(d,p) differs only 2.71 kcal mol^{-1} from the experimental data [8] whereas MP2/6-31+G(d,p) overestimates the barrier by 9.85 kcal mol^{-1}. The 6−311+G(3df,2p) basis set behaves similarly. However, increasing the size of the basis set for M06-2X increases the difference between the calculated and experimental barriers, but leads to the expected improvement for MP2.

The M06−2X/6-31+G(d,p) level agrees best with the experimental reaction enthalpy of Dyer et al. [15]. The aug-cc-pVDZ basis set gives acceptable differences of 2.97 and 2.68 kcal mol^{-1} for M06-2X and MP2, respectively. Thus M06-2X/aug-cc-pVDZ or MP2/aug-cc-pVDZ represent good compromises for the calculations in solution. MP2/aug-cc-pVDZ is probably to be preferred because the basis-set dependence of MP2 is more predictable than that of M06−2X, although the latter is computationally more economical.

Table 4 The computed enthalpies of transition state, TS2 ($\Delta H_{TS2}^{\neq}$) and complex III (ΔH_{III}) relative to complex II in vacuo and dichloroethane

	In vacuo		In dichloroethane	
	$\Delta H_{TS2}^{\neq}$	ΔH_{III}	$\Delta H_{TS2}^{\neq}$	ΔH_{III}
M06−2X/6−31+G(d,p)	10.63	10.77	2.91	−0.36
M06-2X/aug-cc-pVDZ	13.76	11.86	2.98	2.10
MP2/aug-cc-pVDZ	4.79	5.27	−0.45	−2.20

Table 5 Dipole moments (Debye) of the structures in the second step in vacuo

	μ_{II}	μ_{TS2}	μ_{III}
M06−2X/6−31+G(d,p)	4.89	10.95	12.71
MP2/aug-cc-pVDZ	4.96	8.36	9.54

Rearrangement from VH complex II to III

The potential energy surface of the second step including the rearrangement of II to III was generated with coordinate-driving potential scans in which the points on the surface were optimized under constraint of the C-O bond distance (Fig. 2). Scan computations verify that complex II is more stable than III in the gas phase but less stable in solution.

Figure 2 shows two transition states on the potential hypersurfaces. The first one is the third point for both gas and solution phases. The frequency computations of the third points at the same levels were carried out. In solution, the structure calculated for a constrained C-O distance of 1.6 Å has one imaginary frequency for each level. In gas phase, it also has one imaginary frequency for M06-2X/6-31+G(d,p) but no imaginary frequencies for MP2/aug-cc-pVDZ and M06-2X/ aug-cc-pVDZ levels. Therefore, full transition state optimizations of this structure at these levels in gas phase were also carried out. The imaginary frequencies as displacement vectors are shown in Fig. 3, which shows that the structure of the third point cannot be the target transition state for the second step of Vilsmeir-Haack formation since its imaginary frequency does not show the breaking of the C-O bond and the C-Cl bond formation. This transition state belongs to the rotations of N-methyl groups due to steric effect of Cl atom that comes closer to the C atom. Its barrier heights are approximately 6.8-8.2 and 6.2-7.6 kcal mol^{-1} in gas and solution, respectively, which is reasonable for a single bond rotation barrier.

The sixth points (at r_{C-O}=1.9 Å) for the MP2/aug-cc-pVDZ and M06-2X/aug-cc-pVDZ levels and the eighth point (at r_{C-O}=2.1 Å) for M06-2X/6-31+G(d,p) in the gas phase and the fifth points (at r_{C-O}=1.8 Å) for all levels in dichloroethane were identified as the second transition states on the surfaces from the frequency computations. Full optimizations of these points were carried out using the same levels and each gave one imaginary frequency that

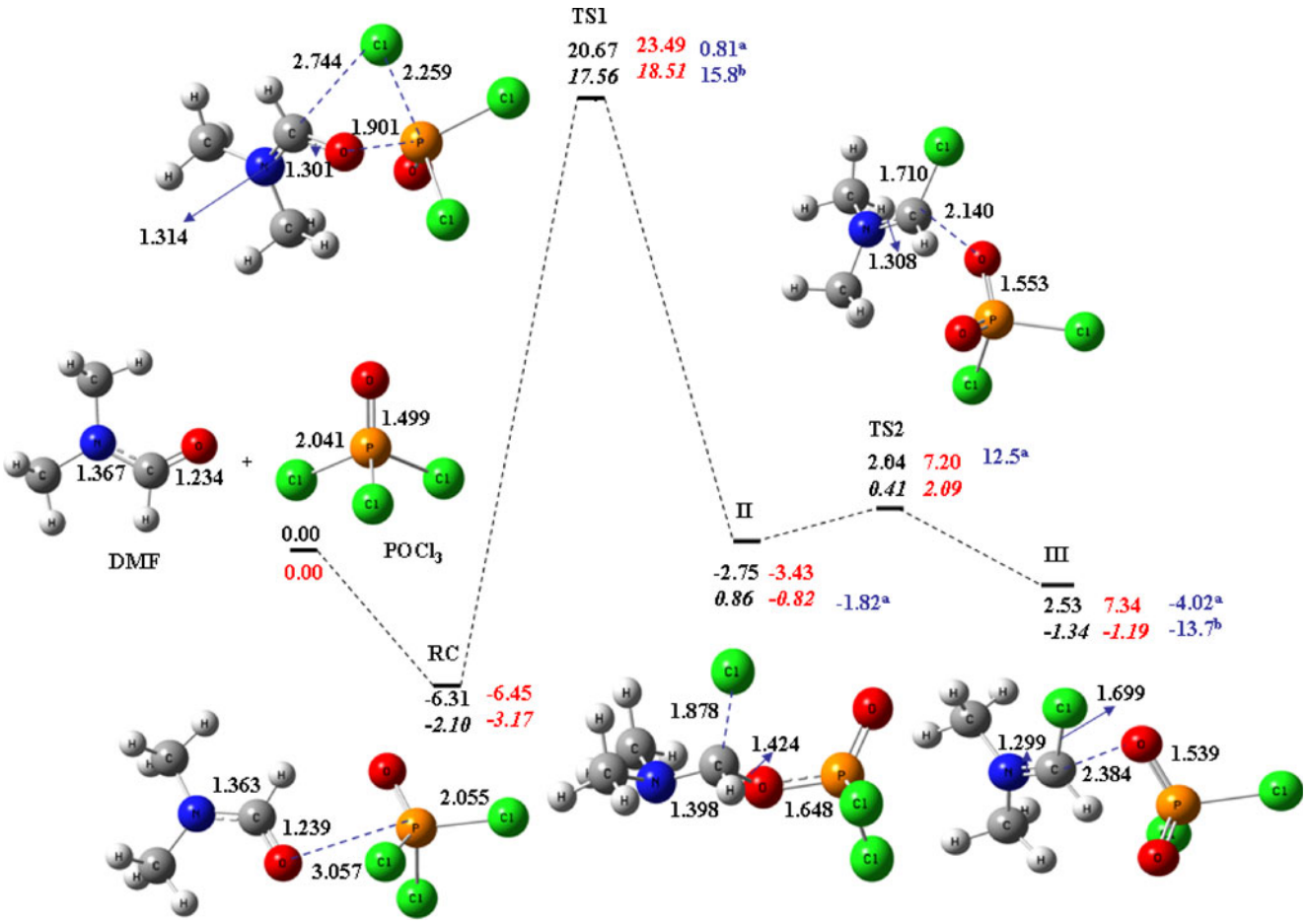

Fig. 4 The reaction path of the Vilsmeier complex formation. The geometric parameters are obtained from full optimized structures with MP2/aug-cc-pVDZ in the gas phase. Relative enthalpies in kcal mol^{-1} are obtained from the MP2/aug-cc-pVDZ (black) and M06-2X/6-31+G(d,p) (red) computations in gas and solution (italic) phases. [a] and [b] : Experimental values (blue) taken from references [15] and [8], respectively

represents the breaking of the C-O bond and the formation of the C-Cl bond (see TS2 in Fig. 1). The reaction and activation enthalpies calculated from full optimizations are listed in Table 4. Single point energy computations in dichloroethane were also performed to calculate solvent effects and these energies were also listed in Table 4.

For the activation energy, M06-2X in gas phase coincidentally agrees well with the reported value (12.47 kcal mol^{-1}) by Dyer et al. [15] but gives a considerably lower value in solution. The activation barriers computed by MP2 in the gas and solution phases are significantly lower than the experimental value and that for $\Delta H_{TS2}^{\neq}$ even becomes negative after vibrational corrections, indicating that the reaction is barrierless at this level. Table 4 shows that the computed activation enthalpies of the second step with M06-2X/6-31+G(d,p) and MP2/aug-cc-pVDZ are lower than the calculated reaction enthalpies. This arises from the fact that complex III has a higher dipole moment than TS2 in the gas phase (Table 5). M06-2X/aug-cc-pVDZ gives a gas phase minimum that is probably spurious. According to the computed reaction energies of the second step, complex II is found to be more stable than III in the gas phase by the levels used, as well as CBS-QB3. On the other hand, in solution phase, the M06-2X/6-31+G(d,p) and MP2/aug-cc-pVDZ find that complex II is less stable than III, which also agrees with CBS-QB3 computations (Table 1), whereas M06-2X/aug-cc-pVDZ still finds complex II more stable than III unlike CBS-QB3. Furthermore, the calculated reaction enthalpy in solution at the M06-2X/6-31+G(d,p) and MP2/aug-cc-pVDZ levels agrees well with the experimental reaction enthalpy (−2.20 kcal mol^{-1}) of Dyer et al. [15].

Figure 4 shows the energy profile of the overall reaction. After full optimizations of the stationary points using the MP2/aug-cc-pVDZ and M06-2X/6-31+G(d,p) levels in the gas phase, the single point energy computations in dichloroethane were also carried out using the same levels. The results obtained from the computations indicate that the second step, which follows first order kinetics, cannot be the rate-determining step of VH complex formation since its barrier is lower than that of the first step in both gas and solution phases. This is not consistent with the observation of Dyer et al. [15], but supports those of Martin et al. [14] and Alunni et al. [8]. However, the computed reaction enthalpy is consistent with reported value (totally, −4.02 kcal mol^{-1}) of Dyer et al. [15].

Conclusions

The above results represent the, to our knowledge, first computational study of the potential energy surface of the Vilsmeier-Haack complex formation mechanism of dimethylformamide (DMF) and phosphorus oxychloride ($POCl_3$). The following conclusions can be drawn:

1 The ionic complex II is more stable than complex III in the gas phase but it is less stable in dichloroethane or dichloromethane solution. This is consistent with the fact that structure III has recently gained in favor on the basis of chemical, spectroscopic, and thermodynamic evidence [8, 11–13].

2 Unlike the observation of Dyer et al. [15], we observed that the VH complex formation follows a second order kinetics since the rate-determining step is the first step, the addition of DMF to $POCl_3$ with an activation barriers of 20.7 and 17.6 kcal mol^{-1} in gas and solution phases, respectively. This supports the observation of Martin et al. [14] and Alunni et al. [8]. Nevertheless, for the total reaction enthalpy, the theoretical results are consistent with the results of Dyer et al. [15].

3 For the first step of the Vilsmeier-Haack complex formation, MP2/aug-cc-pVDZ, M06-2X/aug-cc-pVDZ, and M06-2X/6-31+G(d,p) predicted activation energies very close to that of Alunni et al. [8] in solution. However, the MP2/6-311+G(3df,2p) and M06-2X/aug-cc-PVTZ levels performed the best in the gas phase compared to the reference calculations. The computed reaction enthalpies are in better agreement with the data reported by Dyer et al. [10] than with those of Alunni et al. [8].

4 In the second step, the activation barrier of TS2 computed by M06-2X in the gas phase is consistent with the experimental value reported by Dyer et al. [15] but this value is found to be considerably lower by the computational levels used in solution. The MP2/aug-cc-pVDZ and M06-2X/6-31+G(d,p) levels are in good agreement with CBS-QB3 in the prediction of the stability of VH complexes.

Acknowledgments We thank the Excellence Cluster Engineering of Advanced Materials (funded by the Deutsche Forschungsgemeinschaft) for financial support.

References

1. Vilsmeier A, Haack A (1927) Über die Einwirkung von Halogenphosphor auf Alkyl-formanilide. Eine neue Methode zur Darstellung sekundärer und tertiärer p-Alkylamino-benzaldehyde. Ber 60:119–122. doi:10.1002/cber.19270600118
2. Awad IMA (1992) Studies on the Vilsmeier-haack reaction. Part XIII: Novel heterocyclo-substituted 4, 4′-bi-pyrazolyl dithiocarbamate derivatives. J Chem Technol Biotechnol 56:339–345. doi:10.1002/jctb.280560403
3. Awad IMA, Hassan KM (1990) Studies on the vilsmeier-haack reaction. Part iv. Synthesis and reaction of some 3-methy l-l-

phenyl-4-(acetyl; iminoacetyl and thioacetyl)-2-pyrazolin-5-thione. Phosphorus Sulfur 47:311–317. doi:10.1080/10426509008037983
4. Yokoyama Y, Okuyama N, Iwadate S, Momoi T, Murakami Y (1990) Synthetic studies of indoles and related compounds. Part 22. The Vilsmeier–Haack reaction of N-benzyl-1,2,3,4-tetrahydrocarbazoles and its synthetic application to olivacine and ellipticine. J Chem Soc Perkin Trans 1:1319–1329. doi:10.1039/P19900001319
5. Kiyomi K, Motonobu I, Takeshi K (1971) Thiamine derivatives of disulfide type. XI. Oxidation of dipropyl disulfide with hydrogen peroxide and properties of the products. Chem Pharm Bull 19:2466–2471
6. Chodankar NK, Seshadri S (1985) Studies in the vilsmeier-haack reaction: part XXV—synthesis of 3-hetarylcoumarins by the application of the vilsmeier-haack reaction. Dyes Pigm 6:313–319. doi:10.1016/0143-7208(85)85001-4
7. Awad IMA (1990) Studies in the Vilsmeier-Haack reaction, part VII: Synthesis and reaction of 3-methyl-1-phenyl-4-acetyl hydrazono 2-pyrazoline-5-one(-5-thione). Monatsh Chem 121:1023–1030. doi:10.1007/BF00809252
8. Alunni S, Linda P, Marino G, Santini S, Savelli G (1972) The mechanism of the Vilsmeier–Haack reaction. Part II. A kinetic study of the formylation of thiophen derivatives with dimethylformamide and phosphorus oxychloride or carbonyl chloride in 1,2-dichloroethane. J Chem Soc Perkin Trans 2:2070–2073. doi:10.1039/P29720002070
9. Bosshard HH, Zollinger H (1959) Die Synthese von Aldehyden und Ketonen mit Amidchloriden und VILSMEIER-Reagenzien. Helv Chim Acta 42:1659. doi:10.1002/hlca.19590420527
10. Bredereck H, Gompper R, Klemm K (1959) Säureamid-Reaktionen XVI. Selbstkondensation N.N-disubstituierter Säureamide. Chem Ber 92:1456–1460. doi:10.1002/cber.19590920631
11. Martin GJ, Martin M (1963) Research on the Vilsmeier -Haack reaction. I. Study of the structure of the intermediary complexes by nuclear magnetic resonance. Bull Soc Chim Fr 637-646
12. Arnold Z, Holy A (1962) Synthetic reactions of dimethylformamide. XIV. Some new findings on adducts of the Vilsmeier-Haack type. Collect Czech Chem C 27:2886–2897
13. Fritz H, Oehl R (1971) Synthesen in der Reihe der Indole und Indolalkaloide, XII. Halogen-Sauerstoff-Austausch zwischen Formamidchloriden und Formamiden, nachgewiesen bei der Einführung deuterierter Formylgruppen nach Vilsmeier. Liebigs Ann Chem 749:159–167. doi:10.1002/jlac.19717490118
14. Martin GJ, Poignant S, Filleux ML, Quemeneur MT (1970) Recherches sur la reaction de vilsmeier-haack etude du mecanisme de formation du complexe par des mesures cinetiques en resonance magnetique nucleaire. Tetrahedron Lett 58:5061–5064. doi:10.1016/S0040-4039(00)96986-7
15. Dyer UC, Henderson DA, Mitchell MB, Tiffin PD (2002) Scale-up of a vilsmeier formylation reaction: use of hel auto-mate and simulation techniques for rapid and safe transfer to pilot plant from laboratory. Org Process Res Dev 6:311–316. doi:10.1021/op0155211
16. Frisch MJ, Trucks GW, Schlegel HB, Scuseria GE, Robb MA, Cheeseman JR, Montgomery JA, Vreven T, Kudin KN, Burant JC, Millam JM, Iyengar SS, Tomasi J, Barone V, Mennucci B, Cossi M, Scalmani G, Rega N, Petersson GA, Nakatsuji H, Hada M, Ehara M, Toyota K, Fukuda R, Hasegawa J, Ishida M, Nakajima T, Honda Y, Kitao O, Nakai H, Klene M, Li X, Knox JE, Hratchian HP, Cross JB, Bakken V, Adamo C, Jaramillo J, Gomperts R, Stratmann RE, Yazyev O, Austin AJ, Cammi R, Pomelli C, Ochterski JW, Ayala PY, Morokuma K, Voth GA, Salvador P, Dannenberg JJ, Zakrzewski VG, Dapprich S, Daniels AD, Strain MC, Farkas O, Malick DK, Rabuck AD, Raghavachari K, Foresman JB, Ortiz JV, Cui Q, Baboul AG, Clifford S, Cioslowski J, Stefanov BB, Liu G, Liashenko A, Piskorz P, Komaromi I, Martin RL, Fox DJ, Keith T, Al-Laham MA, Peng CY, Nanayakkara A, Challacombe M, Gill PMW, Johnson B, Chen W, Wong MW, Gonzalez C, Pople JA (2003) Gaussian 03, Revision D.02. Gaussian Inc, Pittsburgh
17. Frisch MJ, Trucks GW, Schlegel HB, Scuseria GE, Robb MA, Cheeseman JR, Scalmani G, Barone V, Mennucci B, Petersson GA, Nakatsuji H, Caricato M, Li X, Hratchian HP, Izmaylov AF, Bloino J, Zheng G, Sonnenberg JL, Hada M, Ehara M, Toyota K, Fukuda R, Hasegawa J, Ishida M, Nakajima T, Honda Y, Kitao O, Nakai H, Vreven T, Montgomery JA, Peralta JE, Ogliaro F, Bearpark M, Heyd JJ, Brothers E, Kudin KN, Staroverov VN, Kobayashi R, Normand J, Raghavachari K, Rendell A, Burant JC, Iyengar SS, Tomasi J, Cossi M, Rega N, Millam JM, Klene M, Knox JE, Cross JB, Bakken V, Adamo C, Jaramillo J, Gomperts R, Stratmann RE Yazyev O, Austin AJ, Cammi R, Pomelli C, Ochterski JW, Martin RL, Morokuma K, Zakrzewski VG, Voth GA, Salvador P, Dannenberg JJ, Dapprich S, Daniels AD, Farkas O, Foresman JB, Ortiz JV, Cioslowski J, Fox DJ (2009) Gaussian 09, Revision A.02. Gaussian Inc, Wallingford
18. Nyden MR, Petersson GA (1981) Complete basis set correlation energies. I. The asymptotic convergence of pair natural orbital expansions. J Chem Phys 75:1843–1862. doi:10.1063/1.442208
19. Petersson GA, Al-Laham MA (1991) A complete basis set model chemistry. II. Open-shell systems and the total energies of the first-row atoms. J Chem Phys 94:6081–6090. doi:10.1063/1.460447
20. Petersson GA, Tensfeldt TG, Montgomery JA Jr (1991) A complete basis set model chemistry. III. The complete basis set-quadratic configuration interaction family of methods. J Chem Phys 94:6091–6101. doi:10.1063/1.460448
21. Baboul AG, Curtiss LA, Redfern PC, Raghavachari K (1999) Gaussian-3 theory using density functional geometries and zero-point energies. J Chem Phys 110:7650–7657. doi:10.1063/1.478676
22. Marenich AV, Cramer CJ, Truhlar DG (2009) Universal solvation model based on solute electron density and on a continuum model of the solvent defined by the bulk dielectric constant and atomic surface tensions. J Phys Chem B 113:6378–6396. doi:10.1021/jp810292n
23. Becke AD (1996) Density functional thermochemistry. IV. A new dynamical correlation functional and implications for exact–exchange mixing. J Chem Phys 104:10401046. doi:10.1063/1.470829
24. Adamo C, Barone V (1997) Toward reliable adiabatic connection models free from adjustable parameters. Chem Phys Lett 274:242–250. doi:10.1016/S0009-2614(97)00651-9
25. Lee C, Yang W, Parr RG (1988) Development of the Colle-Salvetti correlation-energy formula into a functional of the electron density. Phys Rev B 37:785–789. doi:10.1103/PhysRevB.37.785
26. Grimme S (2006) Semiempirical hybrid density functional with perturbative second-order correlation. J Chem Phys 124:034108. doi:10.1063/1.2148954
27. Becke AD (1993) Density-functional thermochemistry. III. The role of exact exchange. J Chem Phys 98:5648–5652. doi:10.1063/1.464913
28. Perdew JP, Burke K, Wang Y (1996) Generalized gradient approximation for the exchange-correlation hole of a many-electron system. Phys Rev B 54:16533–16539. doi:10.1103/PhysRevB.54.16533
29. Perdew JP, Burke K, Ernzerhof M (1996) Generalized gradient approximation made simple. Phys Rev Lett 77:3865–3868. doi:10.1103/PhysRevLett.77.3865
30. Lynch BJ, Truhlar DG (2002) What are the best affordable multi-coefficient strategies for calculating transition state geometries and

barrier heights? J Phys Chem A 106:842–846. doi:10.1021/jp014002x
31. Lynch BJ, Truhlar DG (2002) How well can hybrid density functional methods predict transition state geometries and barrier heights? J Phys Chem A 105:2936–2941. doi:10.1021/jp004262z
32. Zhao Y, Truhlar DG (2008) The M06 suite of density functionals for main group thermochemistry, thermochemical kinetics, noncovalent interactions, excited states, and transition elements: two new functionals and systematic testing of four M06-class functionals and 12 other functionals. Theor Chem Acc 120:215–241. doi:10.1007/s00214-007-0310-x
33. Møller C, Plesset MS (1934) Note on an approximation treatment for many-electron systems. Phys Rev 46:618–622. doi:10.1103/PhysRev.46.618
34. Ditchfield R, Hehre WJ, Pople JA (1971) Self-consistent molecular orbital methods. 9. Extended Gaussian-type basis for molecular-orbital studies of organic molecules. J Chem Phys 54:724–728. doi:10.1063/1.1674902
35. Hehre WJ, Ditchfield R, Pople JA (1972) Self-consistent molecular orbital methods. XII. Further extensions of Gaussian-type basis sets for use in molecular orbital studies of organic molecules. J Chem Phys 56:2257–2261. doi:10.1063/1.1677527
36. McLean AD, Chandler GS (1980) Contracted Gaussian basis sets for molecular calculations. I. Second row atoms, Z=11–18. J Chem Phys 72:5639–5648. doi:10.1063/1.438980
37. Woon DE, Dunning TH Jr (1993) Gaussian-basis sets for use in correlated molecular calculations. 3. The atoms aluminum through argon. J Chem Phys 98:1358–1371. doi:10.1063/1.464303
38. Kendall RA, Dunning TH Jr, Harrison RJ (1992) Electron affinities of the first-row atoms revisited. Systematic basis sets and wave functions. J Chem Phys 96:6796–6806. doi:10.1063/1.462569
39. Clark T, Chandrasekhar J, Spitznagel GW, Schleyer PvR (1983) Efficient diffuse function-augmented basis-sets for anion calculations. 3. The 3-21+G basis set for 1st-row elements, Li-F. J Comput Chem 4:294–301. doi:10.1002/jcc.540040303
40. Frisch MJ, Pople JA, Binkley JS (1984) Self-consistent molecular orbital methods. 25. Supplementary functions for Gaussian basis sets. J Chem Phys 80:3265–3269. doi:10.1063/1.447079
41. Miertus S, Scrocco E, Tomasi J (1981) Electrostatic interaction of a solute with a continuum. A direct utilizaion of ab initio molecular potentials for the prevision of solvent effects. Chem Phys 55:117–129. doi:10.1016/0301-0104(81)85090-2